

Научная статья

УДК 533.9, 533.9...12

DOI 10.25205/2541-9447-2023-18-4-79-93

Frequency Spectrum of Radiation Flux Generated by Beam-Plasma System with Ten Joules Energy Content in Microsecond Pulse

Andrey V Arzhannikov^{1,2}, Stanislav L. Sinitsky^{1,2}, Denis A. Samtsov¹
Petr V. Kalinin^{1,2}, Sergey S. Popov^{1,2}, Magomedrizy G. Atlukhanov¹
Evgeniy S. Sandalov^{1,2}, Vasilii D. Stepanov^{1,2}, Konstantin N. Kuklin¹
Maxim A. Makarov¹

¹Budker Institute of Nuclear Physics SB RAS
Novosibirsk, Russian Federation

²Novosibirsk State University
Novosibirsk, Russian Federation

A.V.Arzhannikov@inp.nsk.su, <https://orcid.org/0000-0002-8074-9737>

D.A.Samtsov@inp.nsk.su, <https://orcid.org/0000-0002-9914-9125>

Abstract

The work reports the achievement of an energy content of 10 J per microsecond pulse in a directed flux of electromagnetic radiation in the frequency range of $\sim 0.2\text{--}0.3$ THz. The flux is generated by a fundamentally new method, which is realized through the pumping of upper-hybrid plasma oscillations in a magnetized plasma column with a relativistic electron beam (REB) and their subsequent transformation into a flux of electromagnetic radiation. In the described experiments at the GOL-PET facility, this method to generate THz radiation is implemented in the following way a beam of electrons with energy $E \sim 0.5$ MeV with a current density of $(1\text{--}2)$ kA/cm² is passing through a magnetized (4 T) plasma column with a density of $10^{14}\text{--}10^{15}$ cm⁻³. By comparing the experimentally measured spectral composition of the radiation flux with the calculated spectrum, it is proved that this process is realized through resonant pumping of the branch of upper-hybrid plasma waves by such beam. A coordinated increase in plasma density and beam current density opens up the prospect of advancement in the generation of multi-megawatt radiation fluxes in the region of one terahertz.

Keywords

relativistic electron beam, plasma, beam-plasma interaction, waves in plasma, THz radiation, megawatt radiation flux

Funding

Part of this work related to measurements of radiation spectral power density was supported by the Russian Science Foundation (project No. 19-12-00250-P).

Acknowledgments

Authors appreciate Timofeev I.V. for discussion of theoretical aspects in solving scientific problem on electromagnetic wave emission from beam-plasma system.

For citation

Arzhannikov A. V., Sinitsky S. L., Samtsov D. A., Kalinin P. V., Popov S. S., Atlukhanov M. G., Sandalov E. S., Stepanov V. D., Kuklin K. N., Makarov M. A. Frequency Spectrum of Radiation Flux Generated by Beam-Plasma System with Ten Joules Energy Content in Microsecond Pulse. *Siberian Journal of Physics*, 2023, vol. 18, no. 4, pp. 79–93. DOI 10.25205/2541-9447-2023-18-4-79-93

© Аржанников А. В., Синицкий С. Л., Самцов Д. А., Калинин П. В., Попов С. С., Атлуханов М. Г., Сандалов Е. С., Степанов В. Д., Куклин К. Н., Макаров М. А., 2023

Частотный спектр потока излучения, генерируемого пучково-плазменной системой с энергосодержанием десять джоулей в микросекундном импульсе

Андрей Васильевич Аржанников^{1,2}, Станислав Леонидович, Синицкий^{1,2}
Денис Алексеевич Самцов¹, Пётр Валериевич Калинин^{1,2}
Сергей Сергеевич Попов^{1,2}, Магомедризы Гаджимурадович Атлукханов¹
Евгений Сергеевич Сандалов^{1,2}, Василий Дмитриевич Степанов^{1,2}
Константин Николаевич Куклин¹, Максим Александрович Макаров¹

¹Институт ядерной физики СО РАН
Новосибирск, Россия

²Новосибирский государственный университет
Новосибирск, Россия

A.V.Arzhannikov@inp.nsk.su, <https://orcid.org/0000-0002-8074-9737>
D.A.Samtsov@inp.nsk.su, <https://orcid.org/0000-0002-9914-9125>

Аннотация

В статье сообщается о достижении энергосодержания 10 Дж в микросекундном импульсе направленного потока электромагнитного излучения в диапазоне частот $\sim 0,2\text{--}0,3$ ТГц. Генерация осуществляется принципиально новым методом, который реализуется за счет накачки верхнегибридных плазменных колебаний в замагниченном плазменном столбе при помощи релятивистского электронного пучка (РЭП) и последующего преобразования этих колебаний в поток электромагнитного излучения. В частности, в описываемых экспериментах, проводимых на установке ГОЛ-ПЭТ, данный метод реализован следующим образом: пучок электронов с энергией $E \sim 0,5$ МэВ и плотностью тока $(1\text{--}2)$ кА/см² проходит через столб замагниченной (4 Тл) плазмы плотностью $10^{14}\text{--}10^{15}$ см⁻³. В ходе сравнения спектрального состава излучения, измеренного экспериментально, с расчетным спектром доказано, что этот процесс реализуется за счет резонансной накачки таким пучком ветви верхнегибридных плазменных колебаний. Таким образом, одновременное увеличение плотности плазмы и плотности тока пучка открывает перспективу развития генерации мультимегаваттных потоков излучения в районе одного терагерца.

Ключевые слова

релятивистский электронный пучок, плазма, пучково-плазменное взаимодействие, волны в плазме, ТГц-излучение, мегаваттный поток излучения

Финансирование

Часть исследования, посвященная измерению спектральной плотности мощности излучения, выполнена за счет гранта Российского научного фонда (проект № 19-12-00250-Р).

Для цитирования

Arzhannikov A. V., Sinitzky S. L., Samtsov D. A., Kalinin P. V., Popov S. S., Atlukhanov M. G., Sandalov E. S., Stepanov V. D., Kuklin K. N., Makarov M. A. Frequency Spectrum of Radiation Flux Generated by Beam-Plasma System with Ten Joules Energy Content in Microsecond Pulse // Сибирский физический журнал. 2023. Т. 18, вып. 4. С. 79–93. DOI 10.25205/2541-9447-2023-18-4-79-93

1. Introduction

Mastering methods to generate electromagnetic radiation in the frequency range 0.1–1.5 THz seems important due to the possibility to use such radiation fluxes in a wide field of practical applications: high-resolution radar systems, control channels suppression of unmanned aerial vehicles, diagnosis of diseases and investigation of biomaterials [1], visualization of hidden objects [2], impact on objects to achieve structural transformations and changes in their functional characteristics [3]. Under these circumstances, the development and creation of powerful sources of electromagnetic radiation in the specified frequency range have become one of the priority tasks of modern physics.

In our opinion, one of the promising approaches for solving the problem of generating powerful radiation fluxes in the frequency range 0.1–0.9 THz is to implement mechanisms of intense beam-plasma interaction [4] and the transformation of beam-generated plasma waves into electromagnetic

waves emerging from the plasma. It is the physical mechanisms that were proposed to explain the bursts of radiation coming from the solar corona [5]. In the case of using electron beams with an energy of ~ 1 MeV at a current scale of 1–10 kA (see [4]), the power of which reaches the gigawatt level, one can expect the generation of THz radiation fluxes with a power scale of tens and even hundreds of MW. Mastering this new method of generating radiation makes it possible to expand significantly the range of applications of high-power radiation fluxes in the frequency range 0.1–1 THz. It is important to emphasize that the use of this beam-plasma mechanism in the terahertz spectral region opens up a unique opportunity to change quickly the frequency in the generated radiation flux of by varying the plasma density.

Experimental studies in this direction were started at the GOL-3 facility at the Budker Institute of Nuclear Physics SB RAS, under conditions of injection of a beam of MeV electrons with a current of 10–15 kA and a duration of 5 μ s into a magnetized plasma column [6]. In these experiments on the relaxation of high-current REB in a plasma with a density of $\sim 10^{14}$ cm $^{-3}$, the laws of radiation emission in the spectral range 0.1–0.5 THz in the direction perpendicular to the magnetic field in the plasma were established [6]. In subsequent experiments carried out on the GOL-PET facility, it was demonstrated that increase of plasma density results in, the emission direction of the radiation flux switches from perpendicular to the axis of the cylindrical plasma column to the direction along its axis [7]. Based on the results of these and further studies, the mechanisms of radiation generation were determined. One of them is the excitation of upper-hybrid plasma oscillations by a beam with their subsequent transformation into a flow of electromagnetic radiation on plasma density gradients with the radiation frequency equal to the frequency of this branch of plasma waves [7; 8]. Another mechanism is realized during a nonlinear process in which two upper-hybrid oscillations merge into one electromagnetic wave with a frequency equal to twice the magnitude of these oscillations [5; 9]. In studies at the GOL-PET facility, the patterns of influence of plasma density gradients on the spectral composition and power of the THz radiation flux generated during beam-plasma interaction were established, and a new mechanism for generation at the electron plasma frequency was discovered. This mechanism states, that in case of regular periodic gradients of plasma density, direct pumping of a branch of electromagnetic oscillations in the plasma by a beam is possible [10–14].

During experiments at this facility, conditions for the effective extraction of the radiation flux propagating along the axis of the beam-plasma system from the plasma through the end of the plasma column into vacuum were found. Moreover, the experiments determined the conditions for the output of this flux from the vacuum chamber through a dielectric polymer window into the atmosphere of the experimental hall [15], where the first series of measurements of the energy content in the radiation flux with a microsecond pulse duration was carried out [16]. Experiments have shown that the high-power density in the radiation flux leads to a reduction in the time of its release into the atmosphere at a level of less than one microsecond, although the generation time in the beam-plasma system reached 3.5 μ s. This phenomenon of shortening the duration of the radiation pulse outgoing in the atmosphere was explained by an surface RF breakdown development on the vacuum side of the exit window on the [17]. Our work is devoted to solve the problem of preventing this RF breakdown and achieving maximum energy content in the flux released into the atmosphere. In addition, to obtain the possibility of a detailed comparison of the spectrum of the generated radiation with the result of the theoretical consideration, experiments were carried out on the output of the radiation flux into the atmosphere when it is obtained under conditions of a plasma column uniform over the cross section. This comparison of experimental and theoretical results is also given in the text of the article.

2. Experimental facility

The series of experiments presented in the article on the generation of terahertz radiation in a beam-plasma system was carried out at the Budker Institute of Nuclear Physics SB RAS using the GOL-PET facility [14–17]. The injection of a beam into a plasma column is realized from the

U-2 accelerator [18], which uses an accelerating diode of a ribbon configuration under conditions of isolation of the cathode-anode gap by a magnetic field. This accelerator provides injection of a beam of electrons with an energy in the range of 0.4-0.8 MeV, an angular divergence of particle velocity of 0.1 rad [19] with a pulse duration of 5 μ s. In the experiments described, the current density of the beam passing through the plasma column had two values: 1 and 2 kA/cm². The beam was injected into a plasma column (see fig. 1) with a diameter of 80 mm and a length of 1.2 meters, held in a solenoid with a corrugated magnetic field with a ratio of the maximum and minimum values of magnetic induction in the corrugations $B_{\max}/B_{\min} = 4.5/3.2$ T. A set of Rogowski coils is used to measure the beam current in various cross-sections of the vacuum chamber as it propagates along its axis. The energy of the beam electrons is determined by measurements of the voltage applied to the accelerator diode. To measure the plasma density, optical diagnostics are used: a Michelson interferometer at a wavelength of 10.5 μ m and a Thomson scattering system at a wavelength of 1.053 μ m. [20; 21].

The described experiments on the generation of THz radiation were focused on achieving of the maximum energy content per pulse in the radiation flux propagating along the facility axis and then escaping into the atmosphere. In this case, the radiation flux released together with the REB from the end of the plasma column was captured in a steel pipe. Next, this flux was reflected from a stainless-steel mirror at an angle of 90° and outgoing into the atmosphere through an output window made of polymethylpentene (TPX), which transmits submillimeter radiation well [22].

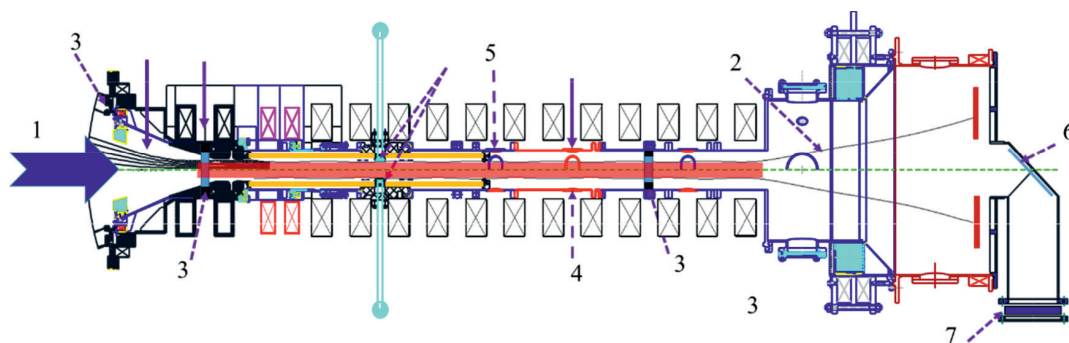


Fig. 1. Schematic drawing of the plasma part of the GOL-PET facility: 1 – electron beam; 2 – magnetic field lines; 3 – Rogowski coil; 4 – Michelson interferometer; 5 – Thomson scattering system; 6 – stainless-steel mirror; 7 – output window

Рис. 1. Схематический чертеж плазменной части установки ГОЛ-ПЭТ:
1 – электронный пучок; 2 – силовые линии магнитного поля; 3 – катушка Роговского;
4 – интерферометр Майкельсона; 5 – система томсоновского рассеяния; 6 – зеркало из нержавеющей стали;
7 – выходное окно

To record the characteristics of the generated submillimeter radiation flux, detectors based on Schottky barrier diodes (SBDs) are used, which are supplemented with frequency-selective bandpass filters. Together, these 8 detectors make up an eight-channel polychromator designed to analyze the spectral composition of the radiation flux in the frequency range from 0.1 to 0.6 THz [23]. To measure the energy content in the EM radiation flux, a specialized calorimeter was used, provided to us by the authors of [24]. The process of measuring radiation energy using a calorimeter is based on the absorption of electromagnetic radiation energy in a thin-walled cylindrical metal-ceramic shell and recording changes in its temperature using a large number (about 1000) of thermocouples connected in series. The sensitivity of the calorimeter, measured at a frequency of about 100 GHz, has a value of 90 μ V/J, which is slightly different from the 70 μ V/J measured at a frequency of 10 GHz, which is indicated in [24]. A description of the measurement procedure and the results of the first series of measurements of the energy content in a pulsed THz radiation flux are given in [16]. Based on the above comment on the calorimeter used, it can be assumed that during the experiments, measurements

of the energy content in the radiation flux in a single pulse are provided with good reliability. Taking the time dynamics and amplitude of the radiation signals in the polychromator channels during the generated pulse, we calculate the absolute value of the average power over the duration of the pulse. To visually indicate the distribution of power density over the cross-section of the radiation flux, which is important for estimating the fraction of the flux captured in the calorimeter, panels of gas-discharge neon bulbs are used. A high-frequency discharge occurs in the bulb cavity when the specific power in the flux exceeds a threshold value, which is estimated at the level $(1-2) \cdot 10^4$ W/cm². A high-frequency discharge that occurs in the cavity of light bulbs evenly distributed over the area of the panel is accompanied by a bright glow, and the optical image of the glow of these light bulbs, recorded using an SDU camera, indicates that the specific flux power exceeds the specified threshold level.

3. Spectral composition of the radiation flux for different plasma density distributions in the plasma column

Taking into account the occurrence of high-frequency electrical breakdown on the surface of the vacuum side of the exit window, through which the radiation flux was released into the atmosphere, to carry out spectral analysis experiments, this window was located at a distance of 180 cm from the stainless-steel mirror. Polymethylpentene has unchangeable transmittance coefficient for EM radiation

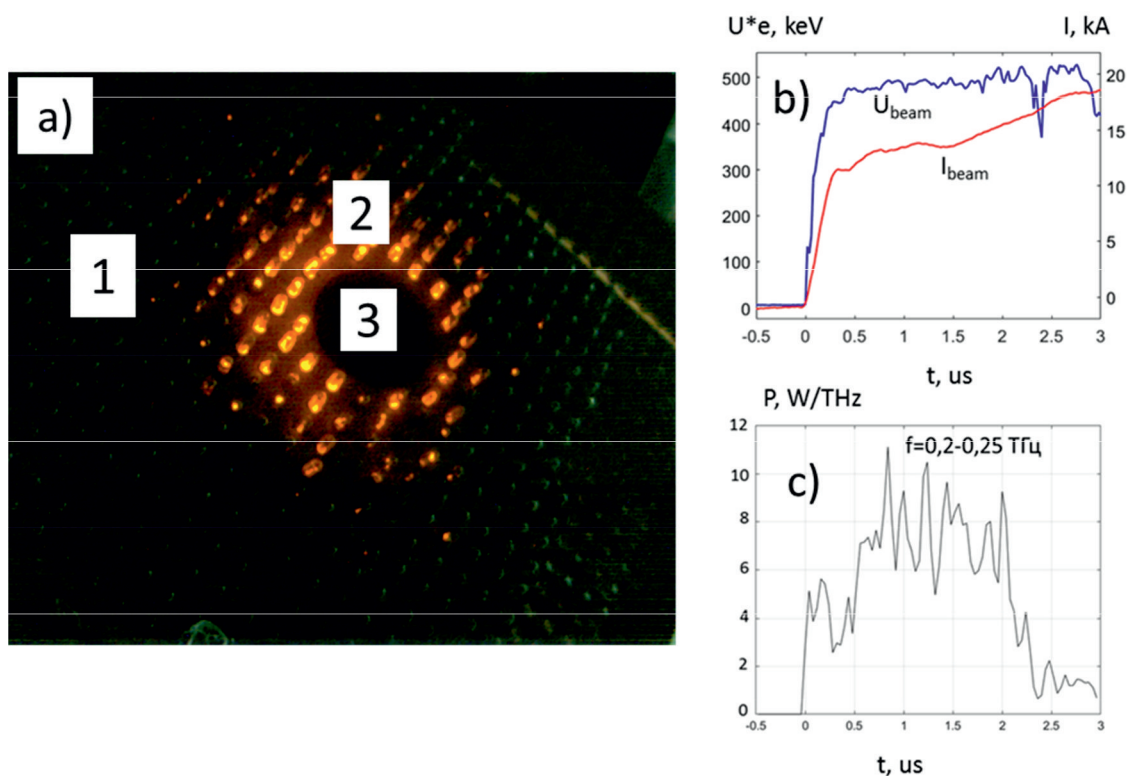


Fig. 2. Panel of the glowing neon bulbs (a) and waveforms of the voltage on the accelerator diode, the beam current passing through the plasma (b), accompanied by signal received from the frequency-selective channel of an 8-channel polychromator (c). 1 – the area of the panel without THz flux; 2 – the area of the panel within THz flux; 3 – the hole in the panel for the polychromator

Рис. 2. Панель светящихся неоновых ламп (a) и осциллограммы напряжения на ускорительном диоде, тока пучка, проходящего через плазму (b), в сопровождении сигнала от частотно-селективного канала 8-канального полихроматора (c). 1 – область панели вне сечения ТГц потока; 2 – область панели внутри сечения ТГц потока; 3 – отверстие в панели для подачи потока на полихроматор

in the studying frequency range. Moreover, this material transmits radiation in the optical region of the spectrum, which makes it possible to control the occurrence of RF breakdown in the vacuum tube where the radiation flux propagates and on the surface of this window. In the path of the radiation flow emerging from the window, a polychromator was installed so that the center of its entrance was located along the axis of the flux coming from the window. Figure 2 shows oscillograms of the voltage on the diode, the beam current passing through the plasma column, and the spectral power density in the frequency range 0.2-0.3 THz, as well as the glow pattern of neon bulbs placed around the entrance hole of the polychromator. From the presented picture of the flux glow on a panel of neon bulbs, it can be seen that the entrance hole of the polychromator, which transmits part of the radiation flux into this device, is localized in the region of maximum radiation power flux density. Moreover, when carrying out measurements, the results of which are presented in this text, the panel with light bulbs in a radiation-absorbing screen having a hole gives a fragment of the radiation flux cross section which with a diameter of 4 cm enters in the operation cavity of the eight-channel polychromator.

This fragment of the flux released in the polychromator operation cavity, having a small angular divergence, upon further propagation in the form of a directed beam, was distributed along the spectral channels of this diagnostic device. Each spectral channel has a calibrated attenuating filter at its input and a detector section with previously measured absolute sensitivity in the spectral range of this frequency-selective channel. Below we provide a description of the results of measurements of the spectral composition of the radiation flux under various experimental conditions.

3.1. The case of a homogeneous distribution of plasma density along the column radius

To carry out the experiments described in this section of the article, such conditions were implemented for the formation of a plasma column under which good homogeneity of the plasma density was achieved in the section of its cross section where the electron beam passes. This ensured the distribution of plasma density along the column axis with minimal possible changes in its value. This made it possible to compare the radiation characteristics measured in the experiment with the results of theoretical analysis, since the theoretical consideration of the problem of the radiation generation spectrum in a beam-plasma system was carried out precisely for this case of plasma density distribution [12]. The results of plasma density measurements using optical laser diagnostics in the described series of experiments are shown in Figure 3. These results were obtained by averaging the recorded signals over a series of 9 shots of the installation under the same experimental conditions.

As one can see in the fig. 3a, which presents the result of measurements using an interferometer at a wavelength of 10.6 μm , the plasma density averaged over the diameter of the plasma column begins to increase sharply from the starting the REB injection. In the time of 0.7 μs the density reaches a value of $5 \cdot 10^{14} \text{ cm}^{-3}$, then its growth slows down significantly, and during the subsequent time up to 2 μs it can be considered at a constant level of $(6 \pm 1) \cdot 10^{14} \text{ cm}^{-3}$. The radial density distribution measured at a time of 1.2 μs using a Thomson scattering system is shown in Figure 3b. The plasma density averaged over the radius of the column was $(7 \pm 0.5) \cdot 10^{14} \text{ cm}^{-3}$, which coincides with the interferometer measurement results within the limits of measurement errors. Considering the fact that these two laser diagnostics, placed in sections of the column that are located at a distance of 22 cm from each other, give almost the same value of plasma density, we can assert that the distribution of plasma density along the length of the plasma column in this section is close to uniform.

Under these experimental conditions with a plasma column uniform in cross-section, measurements were made of the spectral composition of the radiation flux for a given density distribution measured in the frequency range 0.10–0.40 THz. The result of these measurements is presented in Figure 4.

As can be seen from this figure, in this frequency range the increased spectral density of radiation is localized in three areas along the frequency axis. The highest power spectral density was recorded

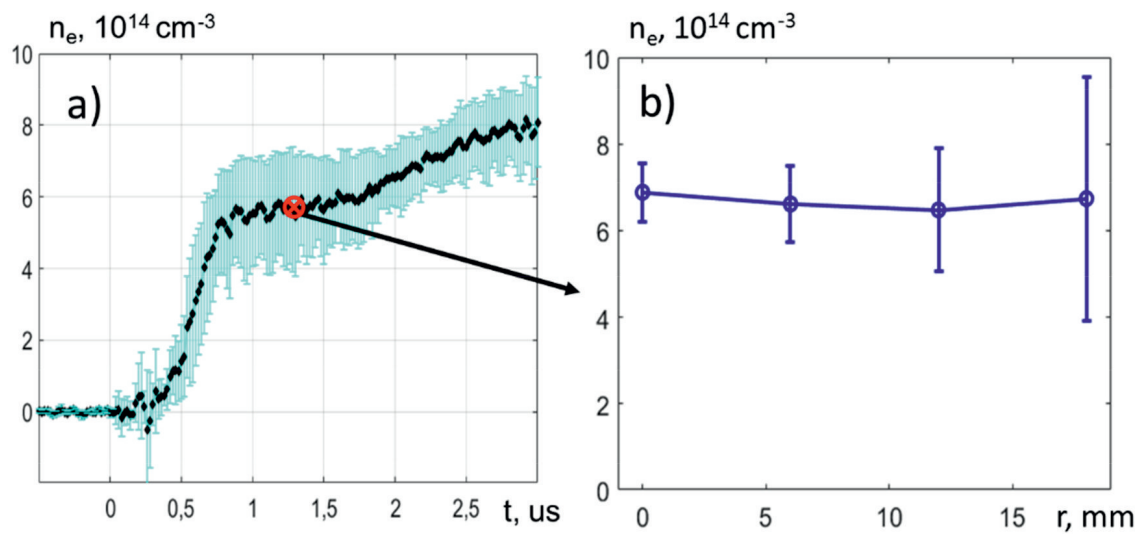


Fig. 3. Change in time of the mean plasma density over the plasma column diameter, recorded using a Michelson interferometer at a wavelength of $10.5 \mu\text{m}$ (a). Plasma density distribution along the column radius in $1.2 \mu\text{s}$ time from starting the beam injection measured by a Thomson scattering system at a laser wavelength of $1.053 \mu\text{m}$ (b)

Рис. 3. Изменение во времени значения плотности плазмы, средней по диаметру плазменного столба, зарегистрированной с помощью интерферометра Майкельсона на длине волны $10,5 \mu\text{м}$ (a).

Распределение плотности плазмы по радиусу столба в момент времени $1,2 \mu\text{с}$ от начала инжекции пучка, измеренное системой томсоновского рассеяния на длине волны лазера $1,053 \mu\text{м}$ (b)

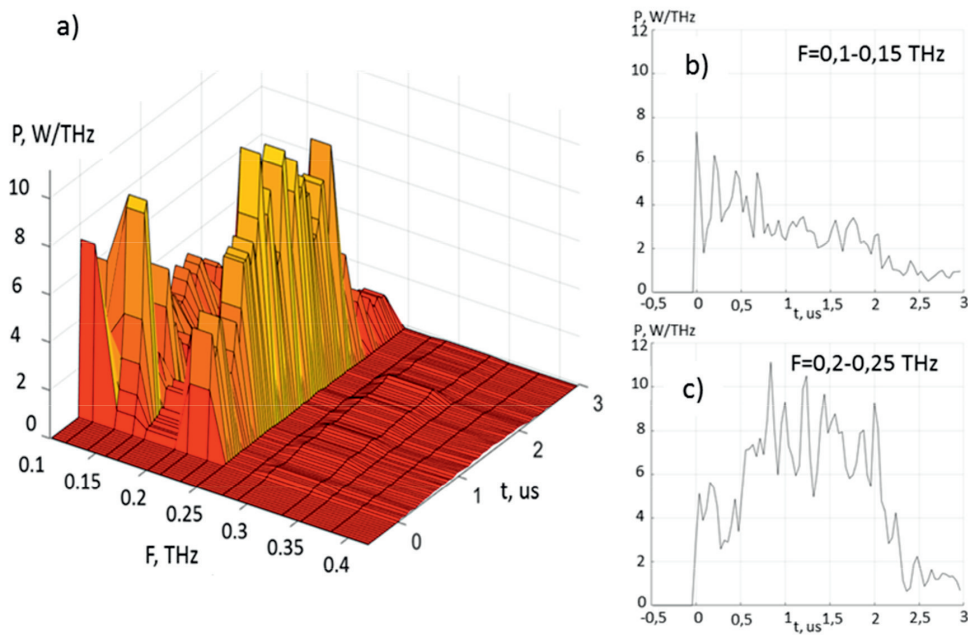


Fig. 4. Spectral power density in the radiation flux generated under conditions of the uniform cross-section of the plasma column (the result was obtained by averaging the recording results over a series of 9 shots under identical experimental conditions with a plasma density distribution shown in Fig. 3, b)

Рис. 4. Спектральная плотность мощности в потоке излучения, генерируемого в условиях однородного по сечению столба плазмы (результат получен усреднением результатов регистрации по серии из 9 выстрелов в одинаковых условиях эксперимента с распределением плотности плазмы, показанным на рис. 3, b)

in the frequency range 0.20–0.25 THz. In this case, a high value of the spectral power density in this spectral interval is maintained for a time from 0.5 to 2 microseconds. Nevertheless, before the start of this period of time with generation in the frequency range 0.20–0.25 THz, there are short (lasting up to 0.5 μ s) bursts of radiation at frequencies 0.12 THz and 0.16 THz with an amplitude comparable to the maximum in the first interval. At higher frequencies relative to the main frequency interval, an increased level of spectral density is observed only in the vicinity of the frequency 0.32 THz, and this increase has an amplitude an order of magnitude lower than the power spectral density in the main radiation peak, localized in the interval 0.20–0.25 THz. We will analyze the distribution of the spectral power density by frequency observed in the experiment within the framework of the theoretical model we have developed under the conditions of the measured experimental parameters.

We associate the relatively high spectral power density in the vicinity of the frequency $f_c = 0.12$ GHz with the movement of electrons along individual cyclotron orbits in a magnetic field with an induction in the vicinity of 4 Tesla. The plasma density of $6 \cdot 10^{14}$ cm⁻³ sets the frequency of Langmuir oscillations $f_p = 0.22$ THz. Taking into account the indicated value of the cyclotron frequency, based on the frequency of Langmuir oscillations, it is possible to calculate the cutoff frequency in the spectrum of upper-hybrid plasma oscillations, which is given by the formula $f_{uh} = \sqrt{f_p^2 + f_c^2}$.

With the indicated experimental parameters, we obtain the cutoff frequency on the branch of upper-hybrid plasma waves $f_{uh} = 0.25$ THz. (see [27]). The result of computer calculations of the spectral composition of radiation emerging from the plasma in the frequency range of upper-hybrid plasma oscillations, performed according to the theoretical model described in [27], is presented in Figure 5a. The result of the calculations is presented here in the form of the distribution of the spectral power density over the angles θ , which is measured from the direction of the magnetic field induction. This result indicates that the radiation generated by the beam propagates at angles of 20-30 degrees to the

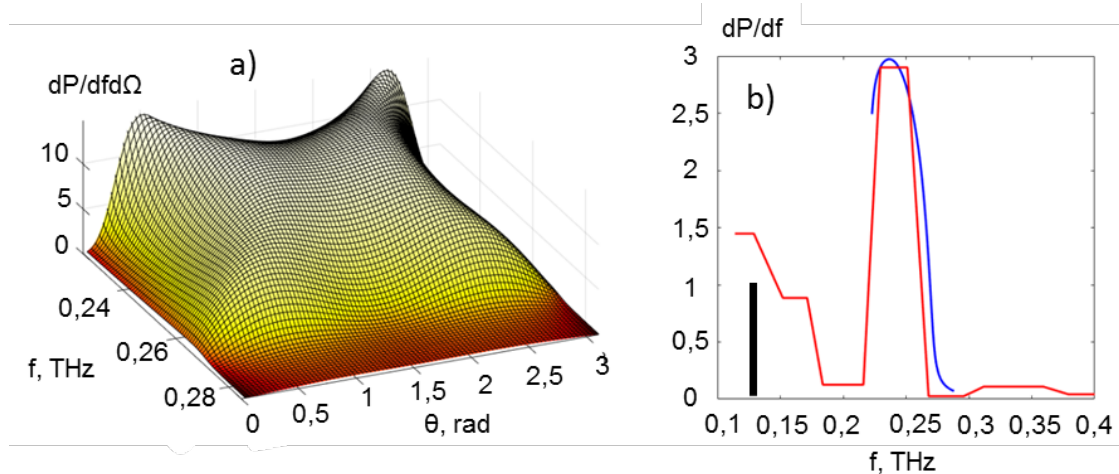


Fig. 5. Distribution of the spectral power density by frequency (in relative units) in the vicinity of the fundamental plasma frequency: calculated angular distribution of the radiation flux in the spectral region near the plasma frequency, which corresponds to the frequency axis unit (a); spectral power density integrated over all angles (b). The blue line is the calculated curve; red line – position of the signal maximum on the frequency axis, recorded by the polychromator in this spectral region; black bold line corresponds to the cyclotron frequency of the plasma electrons

Рис. 5. Распределение спектральной плотности мощности по частотам (в относительных единицах) в окрестности основной плазменной частоты: расчетное угловое распределение потока излучения в спектральной области вблизи плазменной частоты, соответствующей единице оси частот (a); спектральная плотность мощности, интегрированная по всем углам (b). Синяя линия – расчетная кривая; красная – положение максимума сигнала на оси частот, регистрируемого полихроматором в данной области спектра; черная линия соответствует положению циклотронной частоты плазменных электронов

direction of the leading magnetic field. At the same time, the power spectral density integrated over the angles θ is localized in the frequency range 0.22–0.26 THz.

In Figure 5, a comparison is made of the frequency range with a high spectral power density, which was recorded in the experiment for the case of a radiation flux propagating along a magnetic field, with the calculated distribution curve of the spectral radiation density in the flux, obtained in calculations using the above model. A comparison of the results presented in this figure gives grounds for the assertion that the line describing the result of calculating the spectral radiation power density coincides well with the contour covering the region of localization of high values of this parameter, identified from the results of measurements in experiments.

3.2. The case of inhomogeneous plasma density distribution

As was shown in previous series of experiments [14], a decrease in plasma density at a given beam current density helps to increase the power of the generated radiation flux. Moreover, the creation of a plasma column with density gradients along its radius can increase the pulse power several times at fixed values of the average plasma density over the cross section of the column and the current density of the injected beam. A series of experiments aimed at increasing the power in microsecond pulses of THz radiation were carried out this year. During the experiments, the plasma density during the passage of the beam was increase up to a level of $4 \cdot 10^{14} \text{ cm}^{-3}$ with a radial density profile, which is presented in Figure 6. The presented result of measurements of the radial distribution of plasma density by Thomson scattering was obtained by averaging over a series of 5 shots.

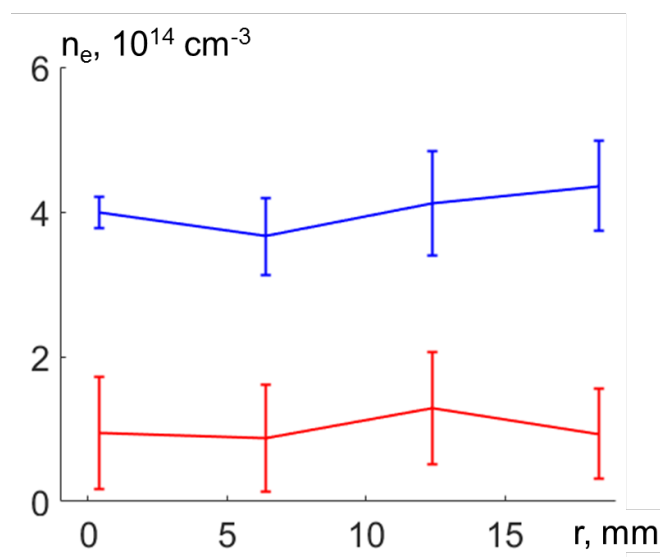


Fig. 6. Density distribution along the radius of the plasma column at a time of 1.5 μs (a) and 3 μs (b).

The result of averaging over five shots under the same conditions for the beam and plasma

Рис. 6. Распределение плотности по радиусу плазменного столба в момент времени 1,5 мкс (a) и 3 мкс (b).

Результат усреднения по пяти выстрелам при одинаковых условиях для луча и плазмы

In the experiments presented here, the current density of the electron beam in the plasma column had a value of about 1 kA/cm². The result of recording the spectral composition of the terahertz radiation flux using an eight-channel polychromator is presented in fig. 7. In the presented radiation spectrum, two frequency regions are distinguished: low-frequency in the range 0.15–0.17 THz and high-frequency 0.30–0.35 THz. In our opinion, the low-frequency region corresponds to the frequency band of upper-hybrid oscillations, and the high-frequency region corresponds to twice the value of

this frequency. The relatively wide spectral frequency range occupied by the marked regions with increased spectral power density can be explained by the presence of variations in the plasma density across the cross section of the plasma column, since the local plasma density determines mainly the frequency of the electron plasma oscillations in this place.

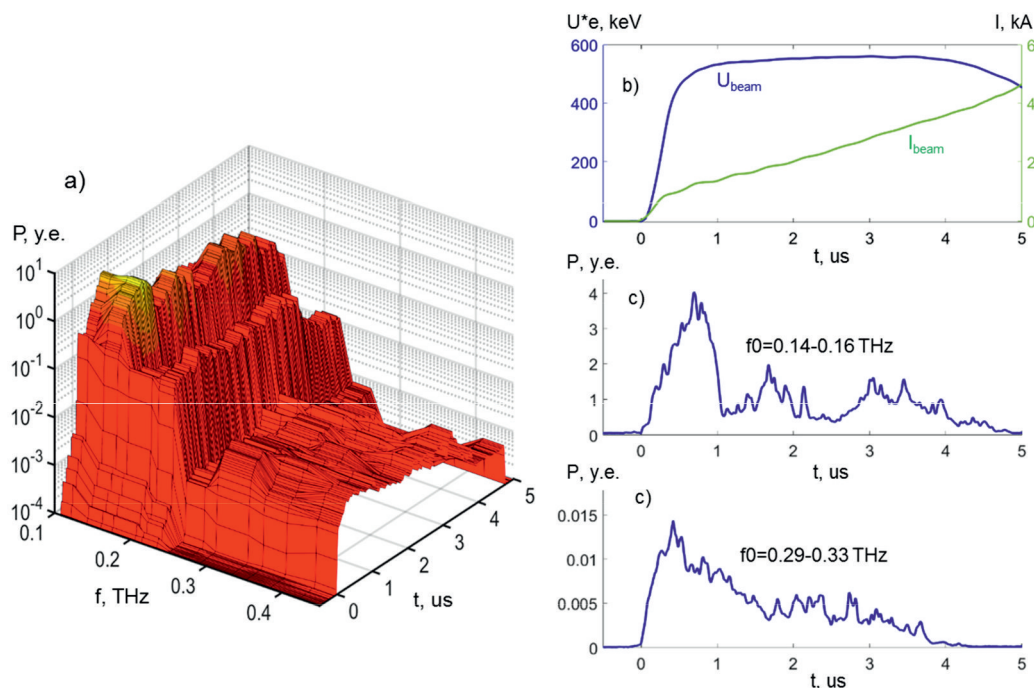


Fig. 7. Spectral radiation power density in the radiation flux released into the atmosphere along the column (a), which was recorded by an eight-channel polychromator in case of the plasma density distribution shown in fig. 6. The ordinate axis shows the spectral radiation power density in relative units in accordance with the calibration of the absolute sensitivity of each channel in its spectral recording region. Voltage and current in the diode (b). Radiation intensity signal received from the polychromator channel in the frequency range 0.14-0.16 THz (c). Signal from the channel in the frequency range 0.29-0.33 THz (d). All signals are averaged over a series of 11 shots

Рис. 7. Спектральная плотность мощности излучения в потоке излучения, выводимого в атмосферу (a), зарегистрированная восьмиканальным полихроматором в случае распределения плотности плазмы, показанном на рис. 6. По оси ординат отложена спектральная плотность мощности излучения в относительных единицах в соответствии с калибровкой абсолютной чувствительности каждого канала в своей спектральной области регистрации. Напряжение и ток в диоде (b). Сигнал интенсивности излучения, полученный из канала полихроматора в диапазоне частот 0,14–0,16 ТГц (c). Сигнал с канала в диапазоне частот 0,29–0,33 ТГц (d). Все сигналы усредняются по серии из 11 снимков

4. Energy content measurements in a radiation flux pulse

The results of previous experiments on measuring the energy content in a pulsed radiation flux are presented in [16]. During those experiments, the calorimeter was located in the atmosphere of the experimental hall, and the radiation flux exited the vacuum chamber through a fluoroplastic window with a diameter of 14 cm. The window was located at a distance of 30 cm from the metal mirror, reflecting the flux that propagates along the axis of the plasma column in a direction perpendicular to this axis. The calorimeter was placed at a distance of 60 cm from the fluoroplastic window, at which the cross-section of the flow freely propagating in the atmosphere already reached a diameter of 0.3 meters. In order to direct the radiation flow to the entrance hole of the calorimeter, which has a diameter of 11.5 cm, a steel pipe with a diameter of 18 cm was placed between the exit window

and the calorimeter, which captured the radiation flow emerging from the exit window. Under these experimental conditions, breakdown along the vacuum surface of the exit window limited the pulse duration of the flow escaping into the atmosphere to a level below $1 \mu\text{s}$. Depending on the detailed experimental conditions, the energy content at this pulse duration turned out to be in the range from $6 \pm 0.5 \text{ J}$ to $9 \pm 2 \text{ J}$.

As noted above, based on the identified reason for the reduction in the pulse duration of the radiation flux escaping into the atmosphere, work was carried out to modify the installation unit in which radiation is extracted from the vacuum into the atmosphere. The fluoroplastic output window was replaced with a window made of polymethylpentene (TPX), and this new window was additionally spaced from the rotating steel mirror at a distance of another 150 cm. To achieve the greatest capture of the radiation flux into the input window of the calorimeter, this input window was attached to the output window from TPH with a minimum gap between them. The layout of the calorimeter and the signal from the calorimeter, averaged over a series of 5 shots, are shown in Figure 8.

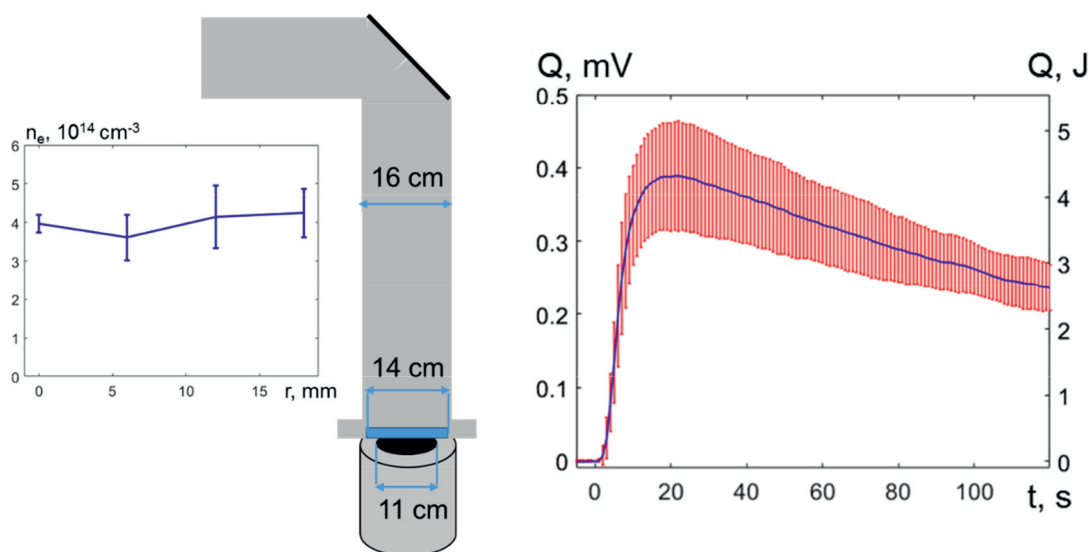


Fig. 8. Measurement results of the energy content in a THz radiation flux of microsecond duration. In this figure are: diagram of the location of the calorimeter behind the exit window of a vacuum tube with a length of 180 cm (a); distribution of plasma density along the radius of the plasma column in the time $2 \mu\text{s}$ (b); the energy content recorded by a calorimeter (c)

Рис. 8. Измерение энергосодержания в потоке ТГц излучения микросекундной длительности.

На рисунке приведены: схема расположения калориметра за выходным окном вакуумной трубы длиной 180 см (a); распределение плотности плазмы по радиусу плазменного столба в момент времени 2 мкс от начала инжекции пучка (b); энергосодержание в импульсе излучения, зарегистрированное калориметром (c)

The next stage of the experiments was the measurement of the energy content in the pulsed radiation flux directly in vacuum. To implement this series of measurements, the window from the TPC was removed, which separated the vacuum of the installation from the air atmosphere of the hall. Under these conditions, the inlet of the working cavity of the calorimeter was a continuation of the tube through which the flow propagates in vacuum after the plane mirror. The calorimeter body was connected to a metal vacuum tube using a dielectric circle, which ensured that there was no electrical contact between the calorimeter body and this tube while maintaining a high vacuum in the calorimeter. Moreover, the inlet of the calorimeter is cut off from the tube through which the flow of THz radiation arrives, using a thin ($100 \mu\text{m}$) film of black polypropylene, which suppresses light and infrared radiation propagating through the tube from the plasma column.

The results of measuring the energy of the radiation flux obtained in this variant of the calorimeter arrangement are presented in Figure 9. On the left half of the figure, indicated by symbol a), the result of measurements carried out under the same conditions as experiments on measuring the energy content in the flux passing through a window of material is presented TPC (see fig. 8, c).

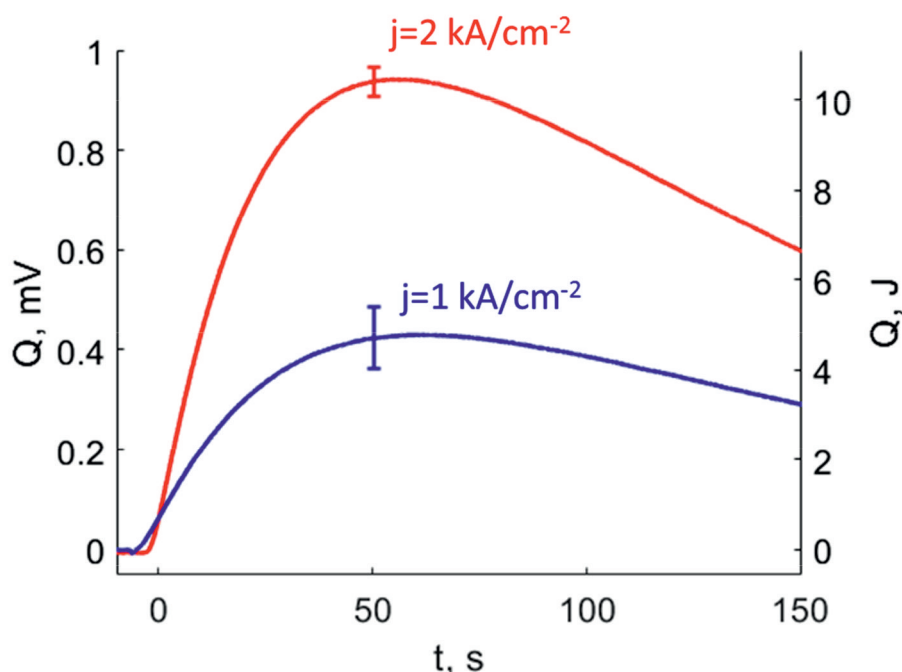


Fig. 9. Energy in a radiation pulse measured in vacuum at various beam current densities in the plasma column: 1 kA/cm² – blue line; 2 kA/cm² – red line

Рис. 9. Энергия в импульсе излучения, измеренная в вакууме при различной плотности тока пучка в плазменном столбе: 1 кА/см² – синяя линия; 2 кА/см² – красная линия

Comparison of the time dynamics of the signals in Fig. 9a and Fig. 8c shows that the temperature rise time of the calorimeter working fluid, which is demonstrated in the figures by voltage oscillograms on thermocouples, in both cases of calorimeter placement has a value of 20-30 seconds. But the characteristic cooling time of the calorimeter working fluid is significantly different for these two options. In the presence of air in the calorimeter cavity, the voltage coming from the thermocouples decreases by half after reaching the maximum signal within 80 seconds, and in the case of a vacuum in the cavity, the voltage signal from the thermocouples decreases during this time on a scale of ten percent. This behavior of the temperature of the working fluid in the calorimeter over time means that the convection of the air mass in its cavity plays a significant role in the removal of energy from the operating calorimeter.

To test the possibility of increasing the intensity of beam-plasma interaction due to an increase in the current density of the injected REB, changes were made to the geometry of the accelerating diode where the ribbon beam is generated. In addition, the values of the magnetic field induction in this diode and the vacuum chamber where the plasma column is created were changed. The magnetic field in the diode was 0.3 T, but became 0.22 T. In turn, for the plasma column was 4.5 T, but became 5 T. Under these conditions, the current density in the beam passing through the plasma column turned out to be increased to 2 kA/cm². The result of measuring the energy content in the radiation flux under conditions of increased beam current density is presented in Fig. 9b.

5. Conclusion

Measurements were carried out of the spectral composition and energy content in the flow of terahertz radiation generated in a magnetized plasma column $(6-7) \cdot 10^{14} \text{ cm}^{-3}$ during relaxation of a pulsed REB of microsecond duration with a current density of level 1–2 kA/cm². During spectral measurements, it was established that the maximum spectral radiation density is localized in the frequency range 0.15–0.3 THz, which coincides with the frequency range of upper-hybrid plasma oscillations, which are effectively pumped under the conditions of the experiments. By selecting the geometry and conditions for calorimetric measurements of the energy content in a powerful radiation flux with a duration of one microsecond, it was possible to determine its level, which reaches ten joules.

References / Список литературы

1. **Markelz A. G., Mittleman D. M.** Perspective on terahertz applications in bioscience and biotechnology // *ACS Photonics*. 2022. Vol. 9, no. 4. P. 1117–1126.
2. **Cooper K. B., Dengler R. J., Llombart N.** [et al.]. THz imaging radar for standoff personnel screening // *IEEE transactions on terahertz science and technology*. 2011. Vol. 1, no. 1. P. 169–182.
3. **Michalchuk A. A. L., Hemingway J., Morrison C. A.** Predicting the impact sensitivities of energetic materials through zone-center phonon up-pumping // *The Journal of Chemical Physics*. 2021. Vol. 154, no. 6. P. 064105.
4. **Arzhannikov A. V., Burdakov A. V., Koidan V. S., Vyacheslavov L. N.** Physics of REB–Plasma Interaction // *Physics of REB–Plasma Interaction. Physica Scripta*. 1982. Vol. 22. P. 303–310.
5. **Ginzburg V. L., Zheleznyakov V. V.** On the Propagation of Electromagnetic Waves in the Solar Corona, Taking Into Account the Influence of the Magnetic Field // *Soviet Astronomy*. 1959. Vol. 3. P. 235–246.
6. **Arzhannikov A. V., Burdakov A. V., Kalinin P. V. et al.** Subterahertz generation by strong langmuir turbulence at two-stream instability of high current 1-MeV REBs // *Vestnik of Novosibirsk State University. Series: Physics*. 2010. Vol. 5, no. 4. P. 44–49.
7. **Arzhannikov A. V., Burdakov A. V., Kalinin P. V. et al.** Properties of sub-THz waves generated by the plasma during interaction with relativistic electron beam // *IRMMW-THz-2015 Conference Proceedings*, TS-3133848.
8. **Timofeev A. V.** Electromagnetic waves in a magnetized plasma near the critical surface // *Phys. Usp.* 2004. Vol. 47. P. 555.
9. **Timofeev I. V., Annenkov V. V., Arzhannikov A. V.** Regimes of enhanced electromagnetic emission in beam-plasma interactions // *Physics of Plasmas*. 2015. Vol. 22. P. 113109. DOI: <http://dx.doi.org/10.1063/1.4935890>
10. **Arzhannikov A. V., Burdakov A. V., Kuznetsov S. A. et al.** Subterahertz emission at strong REB-plasma interaction in multimirror trap GOL-3 // *Fusion Science and Technology*. 2011. Vol. 59, no. 1. P. 74–77.
11. **Arzhannikov A. V., and Timofeev I. V.** Generation of powerful terahertz emission in a beam-driven strong plasma turbulence // *Plasma Physics and Controlled Fusion*. 2012. Vol. 54, no. 10.
12. **Arzhannikov A. V., Burdakov A. V., Burmasov V. S. et al.** Dynamics and spectral composition of subterahertz emission from plasma column due to two-stream instability of strong relativistic electron beam // *IEEE Transactions on terahertz science and technology*. 2016. Vol. 6, no. 2. P. 245–252.
13. **Arzhannikov A. V., Burmasov V. S., Ivanov I. A., et al.** Mechanisms of submillimeter wave generation by kiloampere REB in a plasma column with strong density gradients // *44th Inter-*

- national Conference on Infrared, Millimeter and Terahertz Waves, Paris, 1–6 September 2019 (PID5878973).
14. **Arzhannikov A. V., Ivanov I. A., Kasatov A. A. et al.** Well-directed flux of megawatt sub-mm radiation generated by a relativistic electron beam in a magnetized plasma with strong density gradients // *Plasma Physics and Controlled Fusion*. 2020. Vol. 62, no. 4. P. 045002.
 15. **Samtsov D. A., Arzhannikov A. V., Sinitsky S. L. et al.** Generation of a directed flux of megawatt THz radiation as a result of strong REB-plasma interaction in a plasma column // *IEEE Transactions on Plasma Science*. 2021. Vol. 49, no. 11. P. 3371–3376.
 16. **Arzhannikov A. V., Sinitsky S. L., Popov S. S. et al.** Energy Content and Spectral Composition of a Submillimeter Radiation Flux Generated by a High-Current Electron Beam in a Plasma Column With Density Gradients // *IEEE Transactions on Plasma Science*. 2022. Vol. 50, no. 8. P. 2348–2363.
 17. **Аржанников А. В., Сеницкий С. Л., Самцов Д. А. и др.** Энергосодержание и спектральный состав потока субмиллиметрового излучения с длительностью 5 мкс, генерируемого в плазме при релаксации РЭП // *Физика плазмы*. 2022. Т. 48, № 10. С. 929–936.
 18. **Arzhannikov A. V., Bobylev V. B., Nikolaev V. S. et al.** Ribbon REB research on 0.7 MJ generator U-2 // 9-th Inter. Conf. on High-Power Particle Beams, Washington DC, May 1992. Proceedings. Vol. II: Electron beams. P. 1117–1123
 19. **Arzhannikov A. V., Makarov M. A., Samtsov D. A. et al.** New detector and data processing procedure to measure velocity angular distribution function of magnetized relativistic electrons // *Nuclear Instruments and Methods in Physics Research Section A: Accelerators, Spectrometers, Detectors and Associated Equipment*. 2019. Vol. 942. P. 162349.
 20. **Popov S. S., Vyacheslavov L. N., Ivantsivskiy M. V. et al.** Upgrading of Thomson scattering system for measurements of spatial dynamics of plasma heating in GOL-3 // *Fusion Science and Technology*. 2011. Vol. 59, no. 1. P. 292–294.
 21. **Бурмасов В. С., Бобылев В. Б., Иванова А. А. и др.** Инфракрасный интерферометр для исследования субтермоядерной плазмы в многопробочной ловушке ГОЛ-3 // *Приборы и техника эксперимента*. 2012. № 2. С. 120–123.
 22. **Роголин В. Е., Каплунов И. А., Кропотов Г. И.** Оптические материалы для THz диапазона // *Оптика и спектроскопия*. 2018. Т. 125. № 6. С. 851.
 23. **Arzhannikov A. V., Ivanov I. A., Kuznetsov S. A. et al.** Eight-Channel Polychromator for Spectral Measurements in the Frequency Band of 0.1-0.6 THz // *Proceedings of the 2021 IEEE 22nd International Conference of Young Professionals in Electron Devices and Materials*. IEEE, 2021. P. 101–105.
 24. **Зайцев Н. И., Иляков Е. В., Ковнеристый Ю. К. и др.** Калориметр для измерения энергии мощного электромагнитного импульса // *Приборы и техника эксперимента*. 1992. № 35. С. 153–154.
 25. **Аржанников А. В., Сеницкий С. Л., Старостенко Д. А. и др.** Пучково-плазменный генератор ТГц-излучения на основе индукционного ускорителя (проект ЛИУ-ПЭТ) // *Сибирский физический журнал*. 2023. Т. 18, № 1. С. 28–42.
 26. **Самцов Д. А., Аржанников А. В., Сеницкий С. Л. и др.** Частотный спектр потока излучения в интервале частот 0,1-0,6 ТГц, генерируемого на установке ГОЛ-ПЭТ в различных условиях // *Известия высших учебных заведений. Радиофизика*. 2022. Т. 65, № 5/6. С. 342-352. DOI: https://doi.org/10.52452/00213462_2022_65_05_342
 27. **Аржанников А. В., Тимофеев И. В.** Интенсивное пучково-плазменное взаимодействие как источник субмиллиметрового излучения // *Вестник НГУ. Серия: Физика*. 2016. Т. 11, № 4. С. 78–104.

Информация об авторах

Андрей Васильевич Аржаников, доктор физико-математических наук
Станислав Леонидович Сеницкий, кандидат физико-математических наук
Денис Алексеевич Самцов, младший научный сотрудник
Пётр Валериевич Калинин, научный сотрудник
Сергей Сергеевич Попов, кандидат физико-математических наук
Магомедризы Гаджимурадович Атлуханов, младший научный сотрудник
Евгений Сергеевич Сандалов, научный сотрудник
Василий Дмитриевич Степанов, научный сотрудник
Константин Николаевич Куклин, младший научный сотрудник
Максим Александрович Макаров, ведущий инженер

Information about the Authors

Andrey V. Arzhannikov, Doctor of Physics and Mathematics
Stanislav L. Sinitsky, Doctor of Physics and Mathematics
Denis A. Samtsov, Junior Researcher
Petr V. Kalinin, Researcher
Sergey S. Popov, Doctor of Physics and Mathematics
Magomedrizy G. Atlukhanov, Junior Researcher
Evgeniy S. Sandalov, Researcher
Vasilii D. Stepanov, Researcher
Konstantin N. Kuklin, Junior Researcher
Maxim A. Makarov, Leading Engineer

*Статья поступила в редакцию 27.10.2023; одобрена после рецензирования 11.12.2023;
принята к публикации 11.12.2023*

*The article was submitted 27.10.2023; approved after reviewing 11.12.2023;
accepted for publication 11.12.2023*